

Retrieval of mixing layer depth from existing ceilometer/lidar networks in Europe

M. Haeffelin¹, Y. Morille², U. Górsdorf³, G. Teschke⁴, F. Beyrich³

¹ Institut Pierre-Simon Laplace, Paris, France

² Laboratoire de météorologie dynamique, Palaiseau, France

³ Deutscher Wetterdienst, Lindenberg, Germany

⁴ Hochschule Neubrandenburg, Neubrandenburg, Germany

ABSTRACT

The atmosphere boundary layer is characterized by turbulent fluctuations that induce mixing. The determination of the thickness of the layer in which turbulent mixing occurs is crucial in meteorology to study energy and water fluxes exchanges between the surface and the atmosphere, and in air quality to estimate the concentration of pollutants. It is determined either (1) using temperature, humidity and wind profiles from in-situ vertical profiles or (2) by tracing gradients in atmospheric constituents (aerosols, water vapor) or structures using remotely sensed vertical profiles (lidar, radar, sodar).

Lidars or ceilometers provide vertical profiles of backscatter from aerosol particles. Aerosols are predominantly concentrated in the mixing layer, and hence lidar backscatter signals can be used to trace the depth of the mixing layer. We reviewed more than 20 papers describing methods to retrieve mixing layer depth and find a variety of methods analyzing one-dimensional vertical or temporal gradients in lidar and ceilometer backscatter.

As Lidar/ceilometer data are 3-dimensional in nature (vertical, temporal and intensity), we reviewed 2-dimensional image processing methods. We test and implement a Canny-like 2-D image processing method on 355-nm backscatter lidar data and 905-nm backscatter ceilometer data on both clear and cloudy conditions. We show that this method has a great potential for tracking the mixing layer depth from lidar/ceilometer signals, both in stratified conditions retrieving the stable and residual layers, and in convective conditions retrieving the depth of the developing mixing layer.

We propose to test and implement this new algorithm on a ceilometer network in Europe (e.g. DWD and/or KNMI) to study both temporal and geographical variations of the mixing layer depth.

INTRODUCTION

The atmosphere boundary layer is characterized by turbulent fluctuations that induce mixing. Hence in this report the boundary layer will be referred to as mixing layer. The mixing layer can be defined as the layer in which heat, momentum, gaseous constituents and aerosols are transported from and to the Earth's surface. The mixing layer depth (MLD) defines the top of the layer near the surface where turbulent mixing is occurring (White et al. 2009). As shown in Figure 1, during daytime the mixing layer tends to be unstable as a result of convection and is capped by an entrainment zone. At night a shallow stable layer

forms near the surface in which mixing occurs through intermittent turbulence, leaving a residual layer above. The determination of the depth of daytime and nighttime mixing layers is crucial in meteorology to study energy and water fluxes exchanges between the surface and the atmosphere.

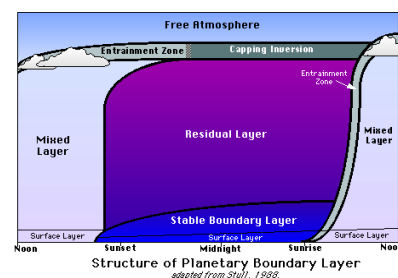


Figure 1. Structure of PBL, from *An Introduction to Boundary Layer Meteorology*, Stull, 1988

Mixing layer depth can be determined either (1) using temperature, humidity, wind and turbulence profiles from in-situ vertical profiles or (2) by tracing gradients in atmospheric constituents or structures using remotely sensed vertical profiles (lidar, wind profiling radar, sodar). This is illustrated in Figure 2. It is important to keep in mind that the (dis)agreement between different retrievals (e.g. temperature based vs aerosol based) is driven to a large extent by the (in)consistency between the atmospheric parameters of interest (potential temperature profile vs aerosol concentration profile).

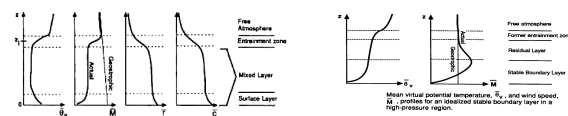


Figure 2. Structure of PBL for convective (left) and stable (right) cases with potential temperature θ_v , wind speed M , water vapor mixing ratio r , and pollutant concentration c from *An Introduction to Boundary Layer Meteorology*, Stull, 1988

Techniques to derive the mixing layer depth (MLD) from thermodynamic vertical profiles date back to the 1970's. Extensive reviews are published on this topic regularly. Similarly methods to diagnostic MLD from model or analyses fields are also well described in the literature. For instance:

- The Parcel method (Holzworth 1972): height of intersection of the actual potential temperature profile with the dry-adiabatic ascent starting at near-surface temperature.

- MLD is also defined as the height where turbulent kinetic energy (TKE) first drops below some fraction of its value at the surface or below some arbitrary lower limit based on experience.
- Others define MLD as the height where the bulk Richardson number for the model outputs surpasses a critical value beyond which the atmosphere is considered decoupled (0.25 Seibert et al., 2000)

Extensive work has also been carried out on analysis of vertical profiles of lidar backscatter to retrieve MLD. Half a dozen different techniques using lidar and/or ceilometer backscatter profiles to retrieve the depth of the boundary layer are published in the literature (see section 3). Most techniques can only be applied on cloud-free boundary layers. Others fail to detect the top of the boundary layer when the lidar or ceilometer signal-to-noise ratio is too low. Methods using vertical gradients may identify several significant gradients making it difficult to identify the location of the MLD. As Lidar/ceilometer data are 3-dimensional in nature (vertical, temporal and intensity), 2-D image processing methods should provide additional retrieval capacity.

Several European countries have started to renew their ceilometer networks with more powerful systems that provide vertical profiles of backscattered power. Hence within a few years, there is great potential for monitoring the height of the mixing layer over the European continent. In preparation for this dataset we propose to test and implement an optimized MLD retrieval algorithm using lidar/ceilometer data from European networks.

MLD RETRIEVALS METHODS WITH LIDAR DATA

Existing 1D methods

We reviewed more than 20 papers describing methods to retrieve mixing layer depth.

Vertical methods

Most of vertical MLD determination methods are based on the estimation of the strongest gradient along the vertical dimension. Those techniques use the first or second derivative of the range-corrected signal Pr_2 or the first derivative of the logarithm of Pr_2 . References: [Flamant et al., 1997,], [Martucci et al., 2007], [Menut et al., 1999], [Sicard et al., 2006]

An other, well described, method is the wavelet covariance technique. The maximum correlation coefficient between the signal and a wavelet is used to detect the MLD. References: [Baars et al., 2008], [Brooks, 2003], [Cohn and Angevine, 2000], [Teschke et al. 2008], [Hajj et al., 2007], [Morille et al., 2007,], [Wauben et al, 2008]

Temporal method

This variance technique is based on the assumption that the top of the boundary layer is the location where the mixing between clean air and ML aerosols is the strongest. References: [Hennemuth and Lammert, 2005], [Hooper and Eloranta, 1986], [Menut et al., 1999]

Proposed Method, STRAT2D

As Lidar/ceilometer data are 3-dimensional in nature (vertical, temporal and intensity), we reviewed 2-D image processing methods. These methods have a great potential for retrieving mixing layer thickness from lidar/ceilometer signals – using both temporal and vertical gradients.

The method presented, called STRAT2D, here is a canny-like edge detection method.

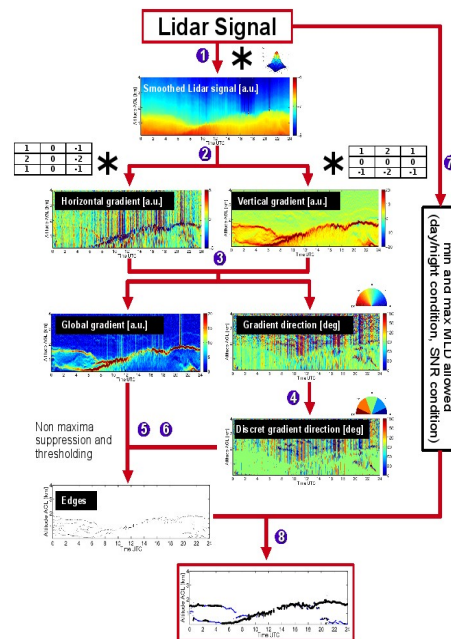


Figure 3. STRAT2D diagram

Canny edge detection (Ref.: [Canny, 1986]) steps are:

1. Smoothing. Before deriving gradients, the signal must be smoothed. Here a gaussian filter is used.
2. Deriving gradients in 2 directions (vertical G_y and horizontal G_x). In our example, Sobel 2D derivating operators (Ref.: [Sobel and Feldman, 1968]) are used
3. Estimating global gradient intensity and direction

$$G = \sqrt{G_x^2 + G_y^2} \quad \theta = \arctan\left(\frac{G_x}{G_y}\right)$$

4. Discretizing global gradient direction
5. NMS (=Non-Maxima Suppression). An edge is determined if the global gradient is local-maximum along its direction
6. Hysteresis thresholding. Two threshold are required T_1 and T_2 ($T_1 < T_2$)

-if (gradient > T_2), edge is kept

-if (gradient < T_1), edge is removed

-if ($T_1 < \text{gradient} < T_2$), edge is kept if connected with gradient > T_2

Steps added to determine the MLD are:

- Estimating the MLD interval allowed with

- SNR condition (i.e. MLD can not be detected in noise)
- day/night condition (for example MLD < 4000m during day, MLD < 2000m during night)
- MLD determination. For each profile, the maximum global gradient on edges is defined to be the MLD.

STUDY DESCRIPTION

Jenoptik CHM 15k ceilometer

The STRAT2D method has been applied on the Jenoptik lidar data implemented at Lindenberg (DWD). This ceilometer model is now used in the DWD ceilometer network. The laser is a diode-pumped Nd:YAG laser emitting at a wavelength of 1064nm. The detection system is a photon-counting detector .

Figure 4 is an illustration of 2 profiles measured the 2008/06/16 at 00:50 UT (blue) and 17:10 UT (black). The first is a clear case and the second is cloudy. Resolutions used in this study are 15m and 30s. As illustrated in this figure, the full overlap can be estimated at a range of 600m above the ground level. This information is very important and can explained the fact that it will be difficult to detect the MLD below this altitude.

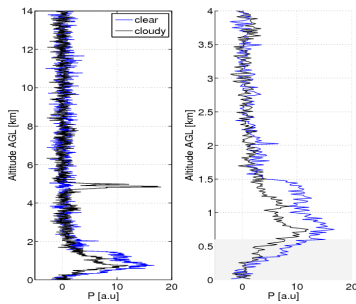


Figure 4. example of 2 ceilometer profiles acquired during the 2008/06/16. the blue one is a clear profile, the black one is cloudy. Altitudes where the overlapping function is not full are shaded in gray.

Another step has been added during this study which allows to determine at each time step which one of the N layers detected seems to be the best estimate. This algorithm developed by Gerd Teschke [Teschke et al. 2008] is based on the fact that the local lidar signal variance due to the noise around the MLD location must differ compared to the total variance of noise.

Dataset

The next table presents a quick view of MLD retrievals available during this study.

Table1: MLD retrievals used for comparisons (*radiosondes retrievals for year 2007 have low quality flag, so only 2008 retrievals will be used, **retrievals not available during this study but can be processed)

Year	Nb of cases	MLD retrievals					
		RS	Jenoptik	Gerd	STRAT2D	MIRA	Model
2007	4	✓*	✓	✓	✓	✓	✓
2008	14	✓	✗**	✗**	✓	✗**	✓

As illustrated in table 1, for the 4 cases of year 2007, 6 retrievals were available:

- "RS": DWD's retrievals from radiosondes data (processed by Frank Beyrich)
- "Jenoptik": Jenotik's retrievals from lidar data
- "Gerd": DWD's retrievals from lidar data (processed by Gerd Teschke [Teschke et al. 2008])
- "STRAT2D": retrievals from 2D algorithm
- "MIRA": DWD's retrievals from cloud radar data [Görsdorf et al. 2009]
- "Model": DWD's retrievals from COSMO EU model

Only radiosondes and model retrievals were available for the 14 cases measured during 2008.

Illustrations

Figures 5 are an example of a comparison obtained during 2007 with the 6 retrievals available.

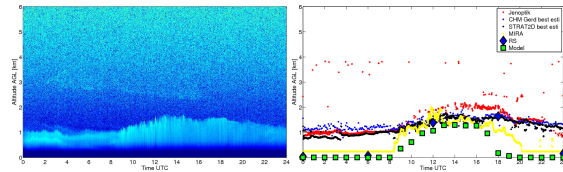


Figure 5. 2007/08/05 ceilometer backscatter and MLD retrievals

Statistical comparisons

The statistical study has been divided in two parts. The first part uses results obtained with cases during 2007 (6 retrieval methods) and the second part uses results obtained during the year 2008 (3 retrieval methods).

Statistical results for the year 2007

Figure 6 shows a comparison between the 2 lidar algorithms (Gerd and STRAT2D) applied on the same ceilometer data. A median filter has been applied on retrievals on a 20min window each 20 minutes for daytime only (between sunrise+2h and sunset-2h) to be sure that MLD is above the ceilometer full overlap range.

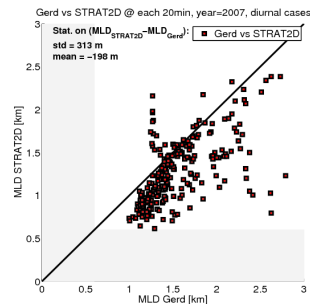


Figure 6. comparison between Gerd and STRAT2D MLD retrievals (year 2007)

This result shows a general good agreement. Discrepancies are quantified as:

1. a bias of 198m with "Gerd" retrievals higher than STRAT2D retrievals. A possible contribution to this bias is that "Gerd" wavelet retrievals identify the MLD in the middle of the

entrainment zone, while STRAT2D retrieves the bottom of the entrainment zone.

2. A standard deviation of 313m. This large value is due in part to situations where the 2 algorithms identify the MLD from 2 distinct layers that can be separated by 1000m or more

As mentioned in table 1, for those 4 cases, MLD retrievals from radiosonde data are not used because they are not all approved by the quality flag.

Statistical results for the year 2008

For this year, MLD retrievals from radiosonde data are all flagged as “good”, and so will be used as our reference.

Figure 7 is a comparison between STRAT2D and radiosonde MLD retrievals separately for launches at 00:00UT, 06:00UT, 12:00UT, and 18:00UT of the 14 cases.

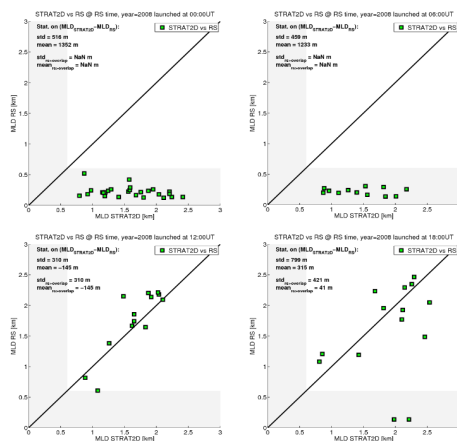


Figure 7. comparison between RS and STRAT2D MLD retrievals (year 2008), separately for launches at 00UT, 06UT, 12UT and 18UT

Those figures show an overall good agreement between STRAT2D and RS MLD retrievals when the MLD is above the ceilometer full overlap altitude:

1. a bias of 59m
2. a standard deviation of 370m

As shown in figures 7 (c) and (d), comparisons with MLD above ceilometer overlap are limited. Figures 7 (a) and (b) show that when the MLD is below the full overlap altitude the gradient detected by STRAT2D is not the MLD but certainly the residual layer.

CONCLUSIONS

Main results obtained are the following:

1. The Jenoptik 1064-nm ceilometer provided aerosol backscatter profiles with high signal-to-noise ratio. While the system is well suited to study the MLD in convective conditions, the full overlap altitude, estimated to be greater than 600m, prevents reliable MLD retrievals in stable boundary layers. A full overlap altitude of 100-200 m is recommended for MLD monitoring.

2. STRAT2D MLD retrievals are compared to radiosonde MLD retrievals during daytime (12 and 18 UT) over an 18-day period. The mean difference is found to be 60 m, which is satisfactory considering that physics at stake is very different. The standard deviation between the two datasets is 370 m, showing that there is little bias, significant discrepancies occur on individual situations. The comparisons must be extended to stable mixing layers (nighttime) using another lidar dataset. Sources of discrepancies between aerosol gradient MLD detected by lidar and thermodynamic MLD detected with radiosonde data should be investigated further.

3. STRAT2D MLD retrievals are also compared to Teschke et al. 1D retrievals over a 4-day period. A bias of 200m is found between the two datasets, which could be attributed in part to the location detected of the entrainment zone. A comparison dataset including stable situations is also necessary to finalize the comparison.

4. The combination of low-altitude Jenoptik 1064-nm ceilometer and the STRAT2D algorithm is an interesting candidate for large scale monitoring of MLD. Other combinations must be investigated, such as Vaisala LD40 or CL31 ceilometer with STRAT2D.

REFERENCES

- [1] Baars et al., ACP, 8, 7281-7296, 2008.
- [2] Brooks, JAOT, 20, 1092 – 1105, 2003.
- [3] Canny, IEEE TPAMI, 8:679-714, 1986.
- [4] Cohn and Angevine, JAM, 39, 1233 – 1247, 2000.
- [5] Eresmaa, et al., ACP, 6, 1485-1493, 2006.
- [6] Flamant et al., BLM, 83, 247–284, 1997 .
- [7] Görsdorf et al., submitted to ISTEP2009 in Delft.
- [8] Haij and Wauben, Scientific Report WR 2007-01, KNMI, De Bilt, 2007.
- [9] Hennemuth and Lammert, BLM, DOI: 10.1007/s10546-005-9035-3, 2005.
- [10] Kizhakkemadam, MofS, The Pennsylvania State University, 2002.
- [11] Hooper and Eloranta, JCAM, 25:990-1000, 1986.
- [12] Martucci et al., JAOT, 24, 1231–1244, 2007.
- [13] Melfi et al., JCAM, 24, 806 – 821, 1985.
- [14] Menut et al., AO, 38, 945-954, 1999.
- [15] Morille et al., JAOT, 24, 761–775, 2007.
- [16] Piironen and Eloranta, JGR, 25 569-25 576, 1995.
- [17] Sicard et al., BLM, 119, 135–157, 2006.
- [18] Sobel and Feldman, G., talk at the Stanford Artificial Project in 1968, unpublished but often cited.
- [19] Steyn et al., JAOT, 16, 953–959, 1999.
- [20] Teschke et al., ILRC Delft, 2008.
- [21] Wauben et al., TECO-2008, 2008.